Electronic structures of square-planar complexes

ARTICLE *in* JOURNAL OF THE AMERICAN CHEMICAL SOCIETY · OCTOBER 1968

Impact Factor: 12.11 · DOI: 10.1021/ja01023a012

Table VII. Ligand-Field Parameters (cm^{-1}) for the Metal Hexacarbonyls

Complex	Δ	B_{cpx}	$B_{free\ ion}$[a]	C	$\beta = B_{cpx}/B_{free\ ion}$
$V(CO)_6^-$	25,500	430	...	1300[b]	...
$Cr(CO)_6$	32,200	520	790	1700[b]	0.66
$Mn(CO)_6^+$	41,050	...	870	2600	...
$Mo(CO)_6$	32,150	380	460	1100	0.83
$W(CO)_6$	32,200	390	370	1300	1.1
$Re(CO)_6^+$	41,000	470	470[c]	1375	1.0

[a] From ref 25. [b] Estimated value. [c] From ref 26.

in the transition from Fe(II) to Co(III) the increased σ bonding destabilizes $3e_g\sigma^*$ to the same extent that $2t_{2g}$ is destabilized by the decreased M→π^*CN bonding; the result is a constant Δ. In the hexacarbonyls, as in $Os(CN)_6^{4-}$ and $Ir(CN)_6^{3-}$,[7] the evidence of increasing Δ values indicates that along an isoelectronic series as above, the σ bonding energetics are affected to a considerably greater extent than the analogous π bonding quantities.

Another effect of interest is the variation of Δ with ligand in an nd^5 or nd^6 series (n = 3–5). Several comparisons are shown in Figure 5. The percentage increase in Δ in going from 3d to 5d valence orbitals again depends on the type of ligand involved. For Cl^-, a very large fractional increase in Δ is observed; a substantial percentage increase in Δ is observed for NH_3, but Δ(CO) in one series actually shows a slight decrease. These observations are consistent with the above analysis, because interelectronic-repulsion effects should decrease in the order 3d > 4d > 5d. Thus, the π-donor ligand is able to move into a better d_σ overlap position as n increases with a resulting destabilization of the $3e_g\sigma^*$ level. The CO ligands, presumably, have already fully exploited the d_σ bonding for the lowest n value and have less to gain in the 4d and 5d series. Indeed, evidence from IP and charge-transfer spectral data (*vide supra*) indicates the $2t_{2g}$ level remains stationary down a series such as $M(CO)_6$ M = Cr, Mo, W). We infer from these data that the d_σ bonding actually decreases, and it is the increased π bonding in carbonyl complexes that holds Δ(4d) and Δ(5d) at values comparable to the Δ(3d) values.

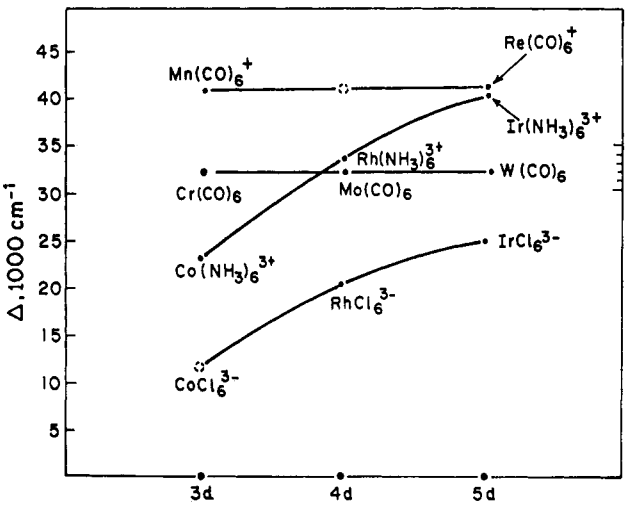

Figure 5. Dependence of Δ on the n quantum number of the d valence orbitals for octahedral complexes.

Acknowledgments. We thank the National Science Foundation for support of this research. Dr. Richard Marsh kindly communicated to us certain pertinent results from the Ph.D. thesis of G. M. Nazarian. We are grateful to Professor D. W. Turner and Dr. D. R. Lloyd for allowing us prepublication access to vertical ionization potential data for the metal hexacarbonyls. We thank Dr. E. Billig for help with the synthesis of $[Mn(CO)_6][BF_4]$ and for several useful discussions.

Electronic Structures of Square-Planar Complexes

W. Roy Mason, III, and Harry B. Gray[1]

Contribution No. 3664 from the Gates and Crellin Laboratories of Chemistry, California Institute of Technology, Pasadena, California 91109.
Received April 19, 1968

Abstract: Electronic spectra of several square-planar complexes of the type $[MX_4]^z$ (M = Pd(II), Pt(II), Au(III); X = Cl^-, Br^-, CN^-, NH_3) are reported in nonaqueous media at room and liquid nitrogen temperatures. In most cases the spectral resolution is considerably enhanced in the rigid, low-temperature glasses. Detailed assignments of spectra measured under carefully controlled conditions allow a comparison of electronic structures and energy levels in the various square-planar systems. The halide complexes show strong ligand→metal charge-transfer absorptions, the cyanides show metal→ligand bands, whereas the ammine complexes exhibit allowed d → p transitions. Trends in d–d and charge-transfer energies are discussed.

Recent investigations of the electronic structures of square-planar complexes indicate that the electronic energy levels vary according to the nature of the ligand.[2-4] The nature of the variation, however, is not presently clear. In view of the several theoretical

(1) Author to whom correspondence should be addressed.

(2) H. B. Gray and C. J. Ballhausen, *J. Am. Chem. Soc.*, **85**, 260 (1963).
(3) C. J. Ballhausen, N. Bjerrum, R. Dingle, K. Eriks, and C. R. Hare, *Inorg. Chem.*, **4**, 514 (1965).
(4) H. Basch and H. B. Gray, *ibid.*, **6**, 365 (1967).

discussions of energy levels in square-planar complexes,[4-7] it is appropriate at this point to emphasize the value of an experimental approach to the question and the need to formulate an experimentally based energy-level scheme for representative types of ligands. Unfortunately, the reliable, high-resolution electronic spectra for square-planar complexes are limited to a few single-crystal studies of low-intensity d–d bands.[3,6,8,9] A number of aqueous solution spectra, particularly those of halide complexes, are subject to question because of the susceptibility of square-planar systems to hydrolysis.[10-13] The charge-transfer spectra of the cationic ammine complexes with halide counterions have not been properly measured because of the strong absorption of the counterions in the same region of the spectrum. Furthermore, careful remeasurement of the spectrum of the $Au(CN)_4^-$ anion has revealed[14] results completely different from those previously reported.[15] All of the bands reported in the previous spectrum were found to be absent, and it is suspected that impure compounds were used for the spectral measurements.

In the present study, detailed spectral measurements are reported for a variety of complexes of palladium(II) and platinum(II) of the type $[MX_4]^s$, where X = halide, cyanide, and ammonia ligands; measurements were made on $Ni(CN)_4^{2-}$ and $Au(NH_3)_4^{3+}$ also. To avoid the possibility of hydrolysis, measurements were made in nonaqueous solvents. Also, where possible, measurements were made in media that form rigid, transparent glasses when cooled to near liquid nitrogen temperature. Low-temperature glasses have advantages over single-crystal measurements; solutions can be made sufficiently dilute so that the intense charge-transfer absorptions can be measured. Also, a solution-like environment is preserved and specific crystal lattice interactions are avoided. Recent measurements on a variety of gold(III) complexes have shown that low-temperature measurements in rigid glasses are quite successful in increasing spectral resolution.[14] The results reported here will be discussed in conjunction with those obtained previously for $AuCl_4^-$, $AuBr_4^-$, and $Au(CN)_4^-$.

Experimental Section

Preparation of Compounds. Starting material for the palladium and platinum complexes was hydrogen tetrachlorometalate(II), H_2PdCl_4 or H_2PtCl_4; the solution was prepared from metal sponge (Englehard Industries).[16,17] The gold complex was prepared from reagent $HAuCl_4 \cdot 3H_2O$ (Mallinckrodt). Tetra-*n*-butylammonium chloride (Eastern Chemical Co.) and bromide (Eastern Organic Chemicals) were used as supplied, without further purification. All other chemicals used were reagent grade. Elemental analyses were performed by Galbraith Laboratories, Inc., Knoxville, Tenn.

Tetra-*n*-butylammonium Tetrachloroplatinate(II), $[(n\text{-}C_4H_9)_4N]_2[PtCl_4]$. A concentrated aqueous solution of H_2PtCl_4 was treated with a 10% less than stoichiometric amount of tetra-*n*-butylammonium chloride. The resulting solution was extracted with chloroform. The chloroform solution was evaporated yielding a thick oil which was dissolved in a small amount of methylene chloride and evaporated first under aspirator vacuum and then under high vacuum to remove the last traces of solvent. A red solid was obtained. *Anal.* Calcd for $[(n\text{-}C_4H_9)_4N]_2[PtCl_4]$: Pt, 23.74; C, 46.77; H, 8.83. Found: Pt, 23.33; C, 47.15; H, 9.08.

Tetra-*n*-butylammonium Tetrabromoplatinate(II), $[(n\text{-}C_4H_9)_4N]_2[PtBr_4]$. An aqueous solution of H_2PtCl_4 was treated with excess concentrated hydrobromic acid and evaporated to a small volume. This process was repeated twice more to expel most of the remaining HCl. A concentrated aqueous solution containing a stoichiometric amount of tetra-*n*-butylammonium bromide was added slowly at ice-bath temperature. A greenish gray precipitate formed immediately, which was collected and washed thoroughly with cold water and then ether, and finally was dried under vacuum. *Anal.* Calcd for $[(n\text{-}C_4H_9)_4N]_2[PtBr_4]$: Pt, 19.52; Br, 31.97; C, 38.45; H, 7.26. Found: Pt, 19.62; Br, 32.07; C. 38.20; H, 7.11.

Tetra-*n*-butylammonium Tetracyanoplatinate(II), $[(n\text{-}C_4H_9)_4N]_2[Pt(CN)_4]$. This compound was prepared from the potassium salt, $K_2Pt(CN)_4$.[18] A concentrated solution of $K_2Pt(CN)_4$ was treated with a 20% less than stoichiometric amount of tetra-*n*-butylammonium chloride. The resulting solution was extracted with an equal volume of methylene chloride. The organic phase then evaporated to dryness yielding a white, powdery solid which was collected and dissolved in a small amount of methylene chloride. The methylene chloride was carefully filtered to remove all insoluble matter and the filtrate was evaporated to dryness. *Anal.* Calcd for $[(n\text{-}C_4H_9)_4N]_2[Pt(CN)_4]$: Pt, 24.88; C, 55.15; H, 9.25; N, 10.72. Found: Pt, 24.65; C, 55.35; H, 9.28; N, 10.91.

Tetraammineplatinum(II) Perchlorate, $[Pt(NH_3)_4](ClO_4)_2 \cdot 2H_2O$. This compound was prepared from the chloride salt, $[Pt(NH_3)_4]Cl_2$,[19] by precipitation with concentrated perchloric acid at ice-bath temperature. *Anal.* Calcd for $[Pt(NH_3)_4](ClO_4)_2 \cdot 2H_2O$: Pt, 39.17. Found: Pt, 38.95.

Tetra-*n*-butylammonium Tetrachloro-μ,μ'-dichloro-dipalladate(II), $[(n\text{-}C_4H_9)_4N]_2[Pd_2Cl_6]$. A concentrated aqueous solution of H_2PdCl_4 was treated with a stoichiometric amount of tetra-*n*-butylammonium chloride as a concentrated aqueous solution. A reddish precipitate was formed immediately which was collected and washed thoroughly with cold water and then ether and finally dried under vacuum. *Anal.* Calcd for $[(n\text{-}C_4H_9)_4N]_2[Pd_2Cl_6]$: Pd, 23.37; C, 42.21; H, 7.97. Found: Pd, 23.15; C, 42.08; H, 8.14.

Tetra-*n*-butylammonium Tetrabromo-μ,μ'-dibromo-dipalladate(II), $[(n\text{-}C_4H_9)_4N]_2[Pd_2Br_6]$. An aqueous solution of H_2PdCl_4 was treated with excess concentrated hydrobromic acid and evaporated to a small volume. This process was repeated twice more to expel most of the remaining HCl. The resulting solution was extracted with a methylene chloride solution containing a 10% less than stoichiometric amount of tetra-*n*-butylammonium bromide. The organic phase was then evaporated to a small volume and cooled. A crystalline product formed and was collected and washed thoroughly with ether and finally dried under vacuum. *Anal.* Calcd for $[(n\text{-}C_4H_9)_4N]_2[Pd_2Br_6]$: Pd, 18.08; C, 32.65; H, 6.16. Found: Pd, 18.05; C, 32.50; H, 6.15.

Several attempts were made to prepare the monomeric tetra-*n*-butylammonium tetrahalopalladate(II) salts; however, only mixtures of the dimeric compounds and excess tetra-*n*-butylammonium halide could be isolated.

Tetra-*n*-butylammonium Tetracyanopalladate(II), $[(n\text{-}C_4H_9)_4N]_2[Pd(CN)_4]$. This compound was prepared from the potassium salt, $K_2Pd(CN)_4$,[20] by the same procedure used for the corresponding platinum compound. *Anal.* Calcd for $[(n\text{-}C_4H_9)_4N]_2[Pd(CN)_4]$: Pd, 15.30; C, 62.18; H, 10.44; N, 12.08. Found: Pd, 14.70; C, 61.60; H, 10.30; N, 11.63.

(5) R. F. Fenske, D. S. Martin, Jr., and K. Ruedenberg, *Inorg. Chem.*, **1**, 441 (1962).
(6) D. S. Martin, Jr., M. A. Tucker, and A. J. Kassman, *ibid.*, **4**, 1682 (1965); as amended, *ibid.*, **5**, 1298 (1966).
(7) F. A. Cotton and C. B. Harris, *ibid.*, **6**, 369 (1967).
(8) O. S. Mortensen, *Acta Chem. Scand.*, **19**, 1500 (1966).
(9) D. S. Martin, Jr., and C. A. Lenhardt, *Inorg. Chem.*, **3**, 1368 (1964).
(10) W. Robb, *ibid.*, **6**, 382 (1967).
(11) M. A. Tucker, C. B. Colvin, and D. S. Martin, Jr., *ibid.*, **3**, 1373 (1964).
(12) J. E. Teggins, D. R. Gano, M. A. Tucker, and D. S. Martin, Jr., *ibid.*, **6**, 69 (1967).
(13) C. M. Harris, S. E. Livingstone, and I. H. Reece, *J. Chem. Soc.*, 1505 (1959).
(14) W. R. Mason and H. B. Gray, *Inorg. Chem.*, **7**, 55 (1968).
(15) A. Kiss, J. Csaszar, and L. Lehotai, *Acta Chem. Acad. Sci. Hung.*, **14**, 225 (1958).
(16) G. B. Kauffman and J. H.-S. Tsai, *Inorg. Syn.*, **8**, 234 (1966).
(17) W. E. Cooley and D. H. Busch, *ibid.*, **5**, 208 (1957).
(18) "Gmelins Handbuch der Anorganischen Chemie," Band 8, Auflage 68c, Verlag Chemie, Weinheim/Bergstrasse, 1939, p 202.
(19) R. N. Keller, *Inorg. Syn.*, **2**, 250 (1946).
(20) J. H. Bigelow, *ibid.*, **2**, 245 (1946).

Tetraamminepalladium(II) Perchlorate, $[Pd(NH_3)_4](ClO_4)_2$. This compound was prepared from the chloride salt $[Pd(NH_3)_4]Cl_2$[21] by precipitation with concentrated perchloric acid at ice-bath temperatures. *Anal.* Calcd for $[Pt(NH_3)_4](ClO_4)_2$: Pd, 28.4. Found: Pd, 28.1.

Tetra-*n*-butylammonium Tetracyanonickelate(II), $[n\text{-}C_4H_9)_4N]_2[Ni(CN)_4]$. A concentrated aqueous solution of potassium tetracyanonickelate(II) ($K_2Ni(CN)_4$)[22] was treated with a 10% less than stoichiometric amount of tetra-*n*-butylammonium bromide and the resulting solution was extracted with chloroform. The organic phase was evaporated to a thick oily liquid which was treated with methylene chloride and evaporated to dryness first under aspirator vacuum and then under high vacuum to remove the last traces of solvent. A faintly yellow powder was obtained. *Anal.* Calcd for $[(n\text{-}C_4H_9)_4N]_2[Ni(CN)_4]$: C, 66.75; N, 12.97; H, 11.20. Found: C, 66.58; N, 12.68; H, 11.41.

Tetraamminegold(III) Perchlorate, $[Au(NH_3)_4](ClO_4)_3 \cdot H_2O$. This compound was prepared from the nitrate salt, which was prepared according to the literature method[23] with the following modification. Concentrated aqueous ammonia was added slowly dropwise to a solution of $HAuCl_4 \cdot 3H_2O$ that was nearly saturated with NH_4NO_3. The pH was never allowed to go over about 5; if the ammonia solution is added too fast or a large excess is used, a yellow precipitate of explosive amido gold complexes is formed. The tetraamminegold(III) nitrate, which crystallizes as ammonia is added, was collected and washed with a minimum amount of ice water and then ether. The salt was reprecipitated by treatment of a strong aqueous solution of the complex with concentrated nitric acid at ice-bath temperatures. *Anal.* Calcd for $[Au(NH_3)_4](NO_3)_3$: Au, 43.66. Found: Au, 43.75.

The perchlorate salt was prepared by dissolving the nitrate in a concentrated aqueous solution of perchloric acid and evaporating at room temperature in the dark under aspirator vacuum. The colorless crystals that were formed were collected and washed with alcohol and ether and dried under reduced pressure in the dark. *Anal.* Calcd for $[Au(NH_3)_4](ClO_4)_3 \cdot H_2O$: Au, 33.88; N, 9.64; H, 2.43. Found: Au, 33.65; N, 9.82; H, 2.33. The salt is sensitive to light, darkening on exposure for more than a short time. All measurements were made on a freshly prepared sample that was carefully protected from light. The complex tends to deprotonate in neutral or slightly alkaline solution giving rise to amido complexes. Therefore, aqueous solution measurements were made in dilute perchloric acid (0.1 *M*).

The preparation and analyses of $[(n\text{-}C_4H_9)_4N][AuCl_4]$, $[(n\text{-}C_4H_9)_4N][AuBr_4]$, and $[(n\text{-}C_4H_9)_4N][Au(CN)_4]$ have been given previously.[14] Some additional spectral measurements were made on these compounds for comparison with the present work.

Spectral Measurements. Spectroquality solvents (Matheson Coleman and Bell) were used wherever possible. Solutions for liquid nitrogen measurements were prepared from EPA solvent (a 5:5:2 mixture of ether, isopentane, and ethanol), a 2:1 mixture of 2-methyltetrahydrofuran and methyl alcohol (2-MeTHF–MeOH), and a 2:1 mixture of 2-methyltetrahydrofuran and propionitrile (2-MeTHF–PN). The 2-methyltetrahydrofuran was chromatoquality reagent (Matheson Coleman and Bell) which had been distilled from sodium to remove all traces of peroxides. The propionitrile (Eastman Organic Chemicals) was purified according to a published method.[24] These three solvent mixtures form rigid transparent glasses at liquid nitrogen temperature. The solvent contraction on cooling to 77°K for EPA has been given as 22.9%.[25] Approximate values for 2:1 2-MeTHF–MeOH and 2:1 2-MeTHF–PN solvent mixtures were determined by cooling a measured volume in a graduated tube to 77°K. The contraction for 2:1 2-MeTHF–MeOH was found to be 21 ± 2% while that for 2:1 2-MeTHF–PN was 20 ± 3%. These latter two contraction values are not precise, but the error introduced into solution concentration is probably less than 5%. The molar extinction coefficients of the spectra reported here have been corrected for solvent contraction using the above values. The near-ultraviolet cutoff points of these three solvent mixtures were found to be as follows: EPA, 47,000 cm^{-1}; 2:1 2-MeTHF–MeOH, 41,000 cm^{-1}; and 2:1 2-MeTHF–PN, 42,000 cm^{-1}.

Spectral measurements were made on a Cary Model 14RI or a Cary Model 15 using 1.00-cm quartz cells. Low-temperature measurements were made with a Cary low-temperature dewar which had been modified to hold a standard 1.00-cm cell. The path-length contraction of a 1.00-cm cell on coolng to 77°K was found to be negligible (0.05–0.1%).

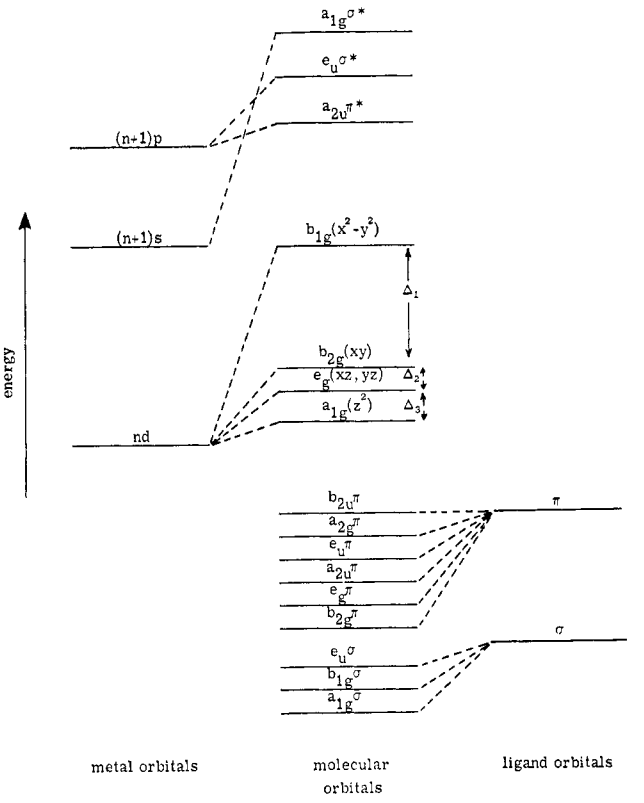

Figure 1. Relative molecular orbital energies for a square-planar (D_{4h}) MX_4^{n-} (X = halide) complex. Only the principal correlation lines are shown.

Molecular Orbital Energy Levels

A generalized molecular orbital energy level diagram adequate for discussion of electronic spectra of square-planar halide and ammine complexes is given in Figure 1. The relative molecular orbital energies are consistent with recent theoretical treatments[4,7] of $PtCl_4^{2-}$. By omitting the levels derived from halide π orbitals, the diagram of Figure 1 may be used as a basis for discussion of electronic spectra of planar ammine complexes.

Figure 2 presents a qualitative energy level scheme for square-planar cyanide complexes. The ordering of σ, π, and π^* CN^- levels is taken from extensive theoretical and experimental studies on octahedral cyanide complexes;[26] relative molecular orbital energies shown for the D_{4h} case are consistent with the spectroscopic data given in this paper.

The complexes considered here all have a d^8 electronic configuration, and the highest filled level of Figures 1 and 2 is $b_{2g}(xy)$. Thus each electronic ground state is $^1A_{1g}$ and is diamagnetic.

Electronic Spectra of Complexes

Square-Planar Halide Complexes. Figure 3 presents the spectrum of the $PtBr_4^{2-}$ anion in 2-MeTHF–PN

(21) H. L. Grube, "Handbook of Preparative Inorganic Chemistry," Vol. III, G. Brauer, Ed., English Translation, Academic Press, New York, N. Y., 1965, p 1585.
(22) W. C. Fernelius and J. J. Burbage, *Inorg. Syn.*, **2**, 227 (1946).
(23) Reference 18, Auflage 62, 1954, p 681.
(24) D. D. Perrin, W. L. F. Armargeo, and D. R. Perrin, "Purification of Laboratory Chemicals," Pergamon Press, New York, N. Y., 1966, p 245.
(25) R. Passerani and I. G. Ross, *J. Sci. Instr.*, **30**, 274 (1953).
(26) J. J. Alexander and H. B. Gray, *J. Am. Chem. Soc.*, **90**, 4260 (1968).

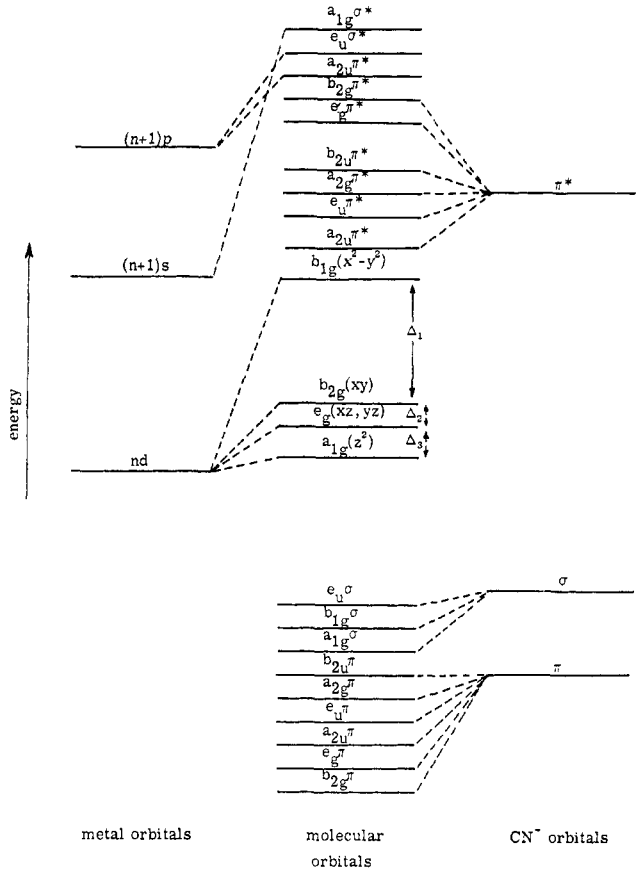

Figure 2. Relative molecular orbital energies for a square-planar (D_{4h}) $M(CN)_4^{n-}$ complex. Only the principal correlation lines are shown.

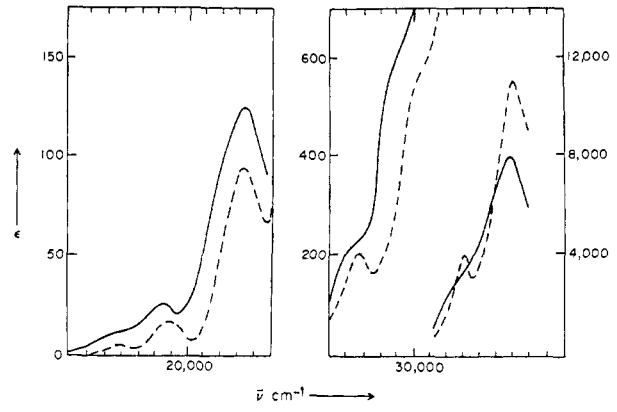

Figure 3. Electronic spectra of $[(n\text{-}C_4H_9)_4N]_2[PtBr_4]$ in 2-MeTHF–PN: ———, 300°K; - - - -, 77°K.

solvent at 300 and 77°K. This spectrum is representative of the spectra of the square-planar halide complexes. The lower energy, weaker bands which are assigned to d → d transitions are seen to decrease in molar extinction on cooling to 77°K, whereas, in contrast, the higher energy allowed bands sharpen and increase in maximum molar extinction. This temperature dependence was found to be characteristic of the measurements reported here. Quantitative spectral data are presented in Table I, together with the assignments of the observed bands. Data and assignments for $AuCl_4^-$ and $AuBr_4^-$ reported previously[14] are also included in Table I for comparison.

The band assignments for the square-planar halide complexes are based on a d MO level ordering of $b_{1g}(x^2 - y^2) > b_{2g}(xy) > e_g(xz, yz) > a_{1g}(z^2)$, in agreement with recent work on $PtCl_4^{2-}$.[4,6,7] Because the $PtCl_4^{2-}$ spectrum will serve as the model, it is well to review the supporting evidence for the assignments in that case. The first spin-allowed d → d transition $b_{2g}(xy) \rightarrow b_{1g}(x^2 - y^2)$ ($^1A_{1g} \rightarrow {}^1A_{2g}$) is believed to occur at 25,000 cm^{-1}. This band is known to be polarized in the xy plane,[9] an observation compatible only with the $xy \rightarrow x^2 - y^2$ assignment. The $xy \rightarrow x^2 - y^2$ transition also is expected to be strongly affected by the in-plane molecular vibrations, and, at liquid helium temperature, the 25,000-cm^{-1} band shows the expected vibrational structure. The assignment of the band observed at 29,700 cm^{-1} as the transition $e_g(xz, yz) \rightarrow b_{1g}(x^2 - y^2)$ ($^1A_{1g} \rightarrow {}^1E_g$) is supported by measurements of magnetic circular dichroism.[27] A small Zeeman splitting is observed which is compatible with a ^1E_g excited state. The designation of the shoulder observed at 37,000 cm^{-1} as the transition $a_{1g}(z^2) \rightarrow b_{1g}(x^2 - y^2)$ ($^1A_{1g} \rightarrow {}^1B_{1g}$) is the least firmly based of the spin-allowed assignments. Recent semiempirical MO calculations[4,7] place the $z^2 \rightarrow x^2 - y^2$ transition in this energy region. The higher molar extinction coefficient observed for this shoulder as compared to the other two spin-allowed bands may be rationalized because of the close proximity of the intense charge-transfer band at about 44,000 cm^{-1}.

The $PtCl_4^{2-}$ spectrum shows at least two weaker bands below 22,000 cm^{-1} as well as a charge-transfer band at about 44,000 cm^{-1}. The weaker bands at about 17,500 and 20,200 cm^{-1} are logically assigned to spin-forbidden d–d transitions. Calculations assuming reasonable values of interelectronic-repulsion parameters have suggested the assignment of these two bands to transitions to the ^3E_g and $^3A_{2g}$ excited states, respectively.[4,6] The charge-transfer band at 44,000 cm^{-1} in acetonitrile has been assigned[2] as ligand→metal (L→M) because the first charge-transfer band in the isoelectronic $AuCl_4^-$ complex is observed at 31,000 cm^{-1} in the same solvent. Such a shift to lower energy on increasing the metal oxidation number is characteristic of a L→M charge-transfer process. The band has been assigned[4] to the transitions $[b_{2u}\pi, e_u\pi] \rightarrow b_{1g}(x^2 - y^2)$.[28]

$PtBr_4^{2-}$. The pattern of absorption bands in the spectrum of $PtBr_4^{2-}$, as shown in Figure 3, is remarkably similar to the one observed in the $PtCl_4^{2-}$ spectrum, although the bands occur at lower energies as expected from the lower position of bromide in the spectrochemical series. The spectral assignments for $PtCl_4^{2-}$ are therefore easily transferred to this case. The two weaker bands at 16,000 and 18,600 cm^{-1} are assigned

(27) D. S. Martin, Jr., G. Foss, M. E. McGarville, M. A. Tucker, and A. J. Kassman, *Inorg. Chem.*, 5, 491 (1966).

(28) In EPA solution at room temperature, a shoulder is observed at 43,670 cm^{-1} (ϵ 8930), while the maximum shifts slightly to 46,300 cm^{-1} (ϵ 11,200). The splitting observed in this solvent is attributed to the separation of the bands due to the transitions originating from the $b_{2u}\pi$ and $e_u\pi$ levels. The shoulder is assigned as $b_{2u}\pi \rightarrow b_{1g}(x^2 - y^2)$ while the maximum is assigned $e_u\pi \rightarrow b_{1g}(x^2 - y^2)$; this ordering of states is assigned because $b_{2u}\pi$ is nonbonding and more intensity is expected for the transition from $e_u\pi$. Better resolution of the $PtCl_4^{2-}$ charge-transfer system is obtained from a spectrum measured on a sample prepared by evaporating a methylene chloride solution of $[(n\text{-}C_4H_9)_4N]_2[PtCl_4]$ to a glassy solid on a Suprasil plate. Two distinct maxima are seen at 42,550 and 45,045 cm^{-1}; as above, the bands are assigned $b_{2u}\pi \rightarrow b_{1g}(x^2 - y^2)$ and $e_u\pi \rightarrow b_{1g}(x^2 - y^2)$, respectively.

Table I. Electronic Spectra of Square-Planar Halide Complexes[a]

CH_3CN	2-MeTHF–PN 300°K	2-MeTHF–PN 77°K	2-MeTHF–MeOH 300°K	2-MeTHF–MeOH 77°K	$^1A_{1g} \rightarrow$
		$[(n\text{-}C_4H_9)_4N]_2[PtCl_4]$			
17.50 (6.5)[b]	17.86 (7.9)[b]	17.86 (3.3)	18.02 (6.4)[b]	18.02 (3.0)	^3E_g
20.24 (16.6)	20.41 (18.2)	20.51 (9.4)	20.45 (16.5)	21.01 (9.3)	$^3A_{2g}$
24.75 (59.6)	24.75 (61.2)	25.19 (33.4)	25.19 (60.5)	25.71 (36.0)	$^1A_{2g}$
29.50 (66.4)	29.72 (79.0)	29.85 (40.8)	29.94 (85.1)	31.25 (63.6)[b]	^1E_g
37.03 (404)[b]	37.04 (427)[b]				$^1B_{1g}$
44.05 (26,900)					$^1A_{2u}$, a ^1E_u
		$[(n\text{-}C_4H_9)_4N]_2[PtBr_4]$			
16.00 (9.3)[b]	16.21 (10.2)[b]	16.21 (5.5)			^3E_g
18.59 (25.0)	18.69 (26.4)	19.01 (16.9)			$^3A_{2g}$
23.15 (126)	23.15 (126)	23.58 (84.6)			$^1A_{2g}$
26.88 (187)[b]	26.52 (221)[b]	26.81 (204)			^1E_g
30.03 (598)[b]	29.67 (640)[b]	30.58 (588)[b]			$^1B_{1g}$
33.33 (3860)[b]	33.11 (3650)[b]	33.00 (4040)			$^1A_{2u}$
36.04 (8400)	35.84 (8100)	36.10 (11,630)			a ^1E_u
47.38 (55,400)					b ^1E_u
		$[(n\text{-}C_4H_9)_4N][AuCl_4]$[c]			
		21.93 (17.3)		21.74 (15.3)	$^1A_{2g}$
25.00 (304)[b]		26.52 (319)[b]	25.00 (334)[b]	26.32 (267)[b]	^1E_g
31.05 (5020)	30.67 (5290)	30.53 (6740)	30.77 (5170)	30.39 (6530)	$^1A_{2u}$, a ^1E_u
44.25 (42,500)					b ^1E_u
		$[(n\text{-}C_4H_9)_4N][AuBr_4]$[c]			
		18.50 (119)[b]	17.80 (170)[b]	18.52 (101)[b]	$^1A_{2g}$
21.74 (1560)[b]	21.60 (1050)[b]	21.32 (1090)	21.74 (1230)[b]	21.23 (1230)	^1E_g
25.25 (4620)	24.88 (3170)	24.94 (4460)	24.88 (3230)	24.81 (4750)	$^1A_{2u}$, a ^1E_u
39.06 (33,200)			39.22 (27,450)	39.68 (29,120)	b ^1E_u
		$[(n\text{-}C_4H_9)_4N]_2[Pd_2Cl_6]$			
		16.29 (11.9)			$^3A_{2g}$
22.20 (350)[b]	22.37 (396)[b]	22.42 (291)			$^1A_{2g}$
24.94 (490)	24.87 (476)	25.16 (403)			^1E_g
30.00 (2100)	29.85 (2380)	30.58 (3310)			$L\pi_B \rightarrow d\sigma^*$
34.70 (2260)	35.21 (2950)[b]	35.21 (3190)			$L\pi_T \rightarrow d\sigma^*$
40.98 (31,200)					$L\sigma_B \rightarrow d\sigma^*$
~50 (~70,000)[b]					$L\sigma_T \rightarrow d\sigma^*$
		$[(n\text{-}C_4H_9)_4N]_2[Pd_2Br_6]$			
		14.60 (15.1)[b]			$^3A_{2g}$
		16.95 (74.8)[b]			$^1A_{2g}$
20.60 (848)[b]	19.61 (780)[b]	19.42 (481)			^1E_g
24.27 (3470)	23.98 (3890)	24.63 (5120)			$L\pi_B \rightarrow d\sigma^*$
30.72 (4470)	30.77 (5050)[b]	30.49 (5610)			$L\pi_T \rightarrow d\sigma^*$
36.76 (36,000)	35.21 (41,400)	35.33 (53,100)			$L\sigma_B \rightarrow d\sigma^*$
46.30 (44,700)[b]					$L\sigma_T \rightarrow d\sigma^*$

[a] $\bar{\nu} \times 10^{-3}$ cm^{-1} (ϵ, l. $mole^{-1}$ cm^{-1}). [b] Shoulder (ϵ is for values of $\bar{\nu}$ given). [c] Measurements in 2-MeTHF–MeOH from ref 14; measurements in 2-MeTHF–PN are from this work.

to spin-forbidden transitions. The first spin-allowed transition, $^1A_{1g} \rightarrow {}^1A_{2g}$, is found at 23,150 cm^{-1} in acetonitrile. The bands at 26,900 and 30,000 cm^{-1} are assigned to the $^1A_{1g} \rightarrow {}^1E_g$ and $^1A_{1g} \rightarrow {}^1B_{1g}$ transitions, respectively. It is noteworthy that the intensity of the d → d spectrum is generally higher for $PtBr_4^{2-}$ than for $PtCl_4^{2-}$. This can be ascribed to increased ligand participation in the *occupied* MO levels derived mainly from the metal d levels. The result of the increased mixing of ligand character in the occupied d levels is increased charge-transfer "character" in the transition to $b_{1g}(x^2 - y^2)$.

The charge-transfer bands at 33,000 and 36,000 cm^{-1} in the $PtBr_4^{2-}$ spectrum correspond to the band at 44,000 cm^{-1} observed for $PtCl_4^{2-}$. Accordingly, they are of the L→M type and are assigned $^1A_{1g} \rightarrow {}^1A_{2u}$ and $^1A_{1g} \rightarrow a\,^1E_u$, respectively. The separation of the $b_{2u}\pi$ and $e_u\pi$ levels is clearly shown in this case. The resolved spectrum at 77°K in 2-MeTHF–PN shows the separation to be 3100 cm^{-1}. In addition, another more intense charge-transfer band is observed at 47,380 cm^{-1} in acetonitrile. This band is assigned to $^1A_{1g} \rightarrow b\,^1E_u$, a transition not observed in the $PtCl_4^{2-}$ spectrum. It is, however, seen in the $AuBr_4^-$ spectrum at 39,000 cm^{-1}. The higher energy in $PtBr_4^{2-}$ than in $AuBr_4^-$ establishes this transition as another L→M process.

$Pd_2Cl_6^{2-}$ and $Pd_2Br_6^{2-}$. In the case of square-planar halide complexes of palladium(II), monomeric tetrahalo complexes could not be isolated as tetra-*n*-butylammonium salts, but instead the planar dimeric halo-bridged complexes,[29] $Pd_2Br_6^{2-}$ and $Pd_2Cl_6^{2-}$, were obtained. There are two types of halide ligands in these complexes, those that are bridging and those which occupy terminal positions. An approximate square plane of halide ligands is maintained around the metal, however, and the d–d transitions which are based mainly on the metal are not strongly affected by the differences in the two types of halides. This is shown from the fact that the d–d band positions of these dimeric complexes are quite similar to those observed in the solid

(29) C. M. Harris, S. E. Livingstone, and N. C. Stephenson, *J. Chem. Soc.*, 3697 (1958).

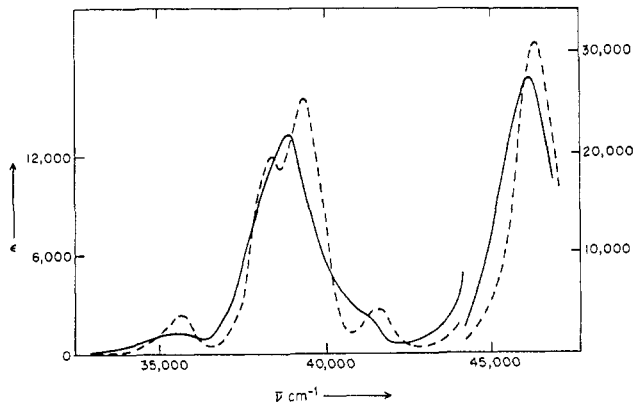

Figure 4. Electronic spectra of $[(n\text{-}C_4H_9)_4N]_2[Pt(CN)_4]$ in EPA: ———, 300°K; – – – –, 77°K.

reflectance and crystal spectra of K_2PdCl_4.[30] The assignment of the lower energy d–d bands given in Table I follows the scheme for the monomeric platinum(II) complexes. The weak bands at 16,300 and 14,600 cm^{-1} resolved in the low-temperature spectra of $Pd_2Cl_6^{2-}$ and $Pd_2Br_6^{2-}$, respectively, are assigned to spin-forbidden transitions.

A more complicated situation arises in the charge-transfer spectra of the dimeric $Pd_2Cl_6^{2-}$ and $Pd_2Br_6^{2-}$ anions. The charge-transfer transitions originate from essentially ligand-based MO levels and are, therefore, sensitive to the electronic environment of the two different types of halide ligands. Since the bridging ligands must contribute electron density to two metal centers, the bonding interaction toward each center will be substantially different from that of the terminal ligands which donate to a single metal center. An analysis of the energy level problem in the lower symmetry (D_{2h}) of the dimeric complexes suggests that the $p\pi$ and $p\sigma$ energy levels of the bridging ligands will be at somewhat higher energy than the corresponding levels arising from the terminal ligands.[31] Therefore, the charge-transfer transitions originating from bridging ligand levels ($L_B \rightarrow M$) should occur at lower energy than those originating from terminal ligand levels ($L_T \rightarrow M$), since the acceptor $b_{1g}(x^2 - y^2)$ level is the same in both cases. Accordingly, the lowest energy charge-transfer band in the spectra of the chloride and bromide complexes at 30,000 and 24,270 cm^{-1}, respectively, is assigned to $L\pi_B \rightarrow d\sigma^*$ transitions. The $L\pi_T \rightarrow d\sigma^*$ transitions in $Pd_2Cl_6^{2-}$ and $Pd_2Br_6^{2-}$ appear at about the same energies as the $^1A_{1g} \rightarrow [^1A_{2u}, a^1E_u]$ transitions in the respective monomeric complexes. At higher energies, the two very intense bands are assigned $L\sigma_B \rightarrow d\sigma^*$ and $L\sigma_T \rightarrow d\sigma^*$; again, the former transition appears lower in energy.

Square-Planar Cyanide Complexes. As a representative example of the electronic spectra of the square-planar cyanide complexes, Figure 4 gives the spectrum of $Pt(CN)_4^{2-}$ at 300 and 77°K in EPA solution. The resolution of the peak at 38,990 cm^{-1} is quite striking. A band in this region had been previously suggested from a curve analysis,[32] but this is the first time it has been clearly demonstrated from resolution at low temperature. Table II contains quantitative spectral data for $Ni(CN)_4^{2-}$, $Pd(CN)_4^{2-}$, and $Pt(CN)_4^{2-}$. The data given for $Pd(CN)_4^{2-}$ near 46,000 cm^{-1} are not very precise because the EPA solvent begins to absorb strongly in this region of the spectrum. Assignments of the observed bands are also given in Table II.

$Pt(CN)_4^{2-}$. All the bands in the $Pt(CN)_4^{2-}$ spectrum are logically assigned to charge-transfer transitions because of their rather high intensities ($\epsilon > 1200$). Furthermore, a comparison of the rich spectrum of $Pt(CN)_4^{2-}$ with the notably empty spectrum of $Au(CN)_4^-$ [14] shows that the charge-transfer bands in the gold(III) complex occur at higher energies than in the platinum(II) complex. This establishes the transitions as metal to ligand ($M \rightarrow L$) charge-transfer processes. It is characteristic of the $M \rightarrow L$ charge-transfer to shift to higher energy on increasing the metal oxidation number, which is in contrast to the shift to lower energy of the $L \rightarrow M$ transitions observed for the square-planar halides. The $M \rightarrow L$ transitions in the tetracyano complexes originate from the occupied d MO levels and terminate on levels derived from the π^* ligand levels. Transitions from the $e_g(xz, yz)$ and $a_{1g}(z^2)$ levels to the lowest π^* level, $a_{2u}\pi^*$ ($^1A_{1g} \rightarrow c^1E_u$ and $^1A_{1g} \rightarrow {}^1A_{2u}$, respectively) are both allowed, but the transition from the $b_{2g}(xy)$ level to $a_{2u}\pi^*$ ($^1A_{1g} \rightarrow {}^1B_{1u}$) is orbitally forbidden. This latter transition should be weaker than the former two. Furthermore, the c^1E_u state may be split by distortions which lower the symmetry from D_{4h}. Using these ideas, the first three bands of the $Pt(CN)_4^{2-}$ spectrum are assigned to the transitions to $^1A_{2u}$, c^1E_u, and $^1B_{1u}$ excited states, respectively.[2] Ion pairing in the solvent would probably cause a sufficient distortion of the $Pt(CN)_4^{2-}$ complex to split the c^1E_u state by the small amount observed.

There is another more intense band in the $Pt(CN)_4^{2-}$ spectrum at higher energy (46,000 cm^{-1}). This charge-transfer transition is also logically assigned as $M \rightarrow L$, and it is presumed to originate from the $b_{2g}(xy)$ occupied d level and terminate on the next higher π^* cyanide level, $e_u\pi^*$. Therefore, the assignment of this band is $^1A_{1g} \rightarrow d^1E_u$. In contrast to the transition from the $b_{2g}(xy)$ level to the $a_{2u}\pi^*$ cyanide level, this transition is fully allowed.

The weaker ligand-field transitions are expected to be at quite high energy in the case of $Pt(CN)_4^{2-}$, because of the high position of the cyanide ligand in the spectrochemical series and the very large d-orbital splitting characteristic of third-row transition metal ions.

$Ni(CN)_4^{2-}$. The spectrum of $Ni(CN)_4^{2-}$ contains a weak shoulder at about 22,500 cm^{-1} ($\epsilon \sim 2$). The remaining bands are considerably more intense. Therefore, it is reasonable to assign this weak shoulder to a spin-forbidden transition. At higher energy, there is a shoulder at about 30,500 cm^{-1} which has been assigned to a d–d transition.[2] Spectra in single crystals have been measured in this region; it appears[3] that d–d excitations are accompanied by substantial changes in equilibrium internuclear configuration symmetry. The band maxima at 32,000, 34,000–35,000, and 36,000–37,000 cm^{-1} are more intense and are assigned as $M \rightarrow L$

(30) P. Day, A. F. Orchard, A. J. Thomson, and R. J. P. Williams, *J. Chem. Phys.*, **42**, 1973 (1965).

(31) A detailed molecular orbital analysis of these and related dimeric D_{2h} systems has been completed and will be published separately by H. B. Gray, W. R. Mason, D. A. Elliot, M. L. S. Ledbetter, and S. L. Laiken; we present relevant experimental data here for comparison with the monomeric tetrahalo complexes.

(32) C. K. Jørgensen, "Absorption Spectra and Chemical Bonding," Addison Wesley Publishing Co., Reading, Mass., 1962, p 198.

Table II. Electronic Spectra of Square-Planar Cyanide Complexes[a]

H_2O[b]	CH_3CN	EPA (300°K)	EPA (77°K)	$^1A_{1g} \rightarrow$
		$[(n\text{-}C_4H_9)_4N]_2[Ni(CN)_4]$		
22.50 (2.0)[c]	22.73 (2.1)[c]			$^3A_{2g}$
30.50 (434)[c]	30.30 (525)[c]	30.77 (558)[c]	31.25 (530)[c]	$^1A_{2g}$
32.26 (703)	31.64 (796)	31.95 (773)	32.15 (838)	$^1B_{1u}$
34.97 (4470)	34.19 (3500)	34.66 (3971)	34.84 (6233)	$^1A_{2u}$
37.30 (12,000)	36.23 (11,350)	36.76 (11,370)	36.23 (5230)[c]	c^1E_u
			37.24 (15,230)	
50.50 (23,000)				d^1E_u
		$[(n\text{-}C_4H_9)_4N]_2[Pd(CN)_4]$		
41.66 (1100)	41.10 (1100)[c]	41.66 (1340)[c]	41.41 (1260)	$^1A_{2g}$
			42.92 (1200)[c]	^1B_u
45.45 (6800)	44.64 (6570)[c]	45.04 (7900)[c]	44.31 (5700)[c]	c^1E_u
			45.09 (9800)	
47.17 (8400)	46.73 (11,800)		46.19 (9200)	$^1A_{2u}$
49.00 (10,400)	47.60 (10,700)[c]			d^1E_u
		$[(n\text{-}C_4H_9)_4N]_2[Pt(CN)_4]$		
35.70 (1270)	35.34 (1270)	35.59 (1800)	35.60 (2430)	$^1B_{1u}$
39.00 (9000)	38.31 (13,200)	38.83 (13,420)	38.39 (11,950)	c^1E_u
			39.25 (15,460)	
41.30 (1300)[c]	40.50 (1820)[c]	40.98 (2470)[c]	41.41 (2740)	$^1A_{2u}$
46.19 (18,700)	45.45 (29,400)	45.87 (28,000)	46.19 (32,200)	d^1E_u
		$[(n\text{-}C_4H_9)_4N][Au(CN)_4]$[d]		
>54.00	>54.00			

[a] $\bar{\nu} \times 10^{-3}$ cm^{-1} (ϵ, l. mole^{-1} cm^{-1}). [b] For $K_2M(CN)_4$. [c] Shoulder (ϵ is for value of $\bar{\nu}$ given). [d] From ref 14.

charge-transfer transitions. Using the scheme for assigning charge-transfer bands as in the case of $Pt(CN)_4^{2-}$, the assignments are $^1A_{1g} \rightarrow {}^1B_{1u}$, $^1A_{1g} \rightarrow {}^1A_{2u}$, and $^1A_{1g} \rightarrow c^1E_u$, respectively. Consistent with this ordering, a small shoulder on the band at 36,000–37,000 cm^{-1} is resolved at low temperature which indicates splitting of the c^1E_u excited state as in the case of $Pt(CN)_4^{2-}$. The fact that the observed splitting is comparable to that found for the c^1E_u state in $Pt(CN)_4^{2-}$ is evidence that a nonspecific, ion-pairing "distortion" mechanism is operable. A charge-transfer band at 50,500 cm^{-1} is also observed in the aqueous solution spectrum of $Ni(CN)_4^{2-}$; in analogy to the band observed at 46,000 cm^{-1} for $Pt(CN)_4^{2-}$, this band is assigned to the $^1A_{1g} \rightarrow d^1E_u$ transition.

$Pd(CN)_4^{2-}$. The spectrum of $Pd(CN)_4^{2-}$ is more difficult to interpret because of the poorer resolution and higher energies of the observed bands. The low-temperature spectrum in EPA indicates the presence of two shoulders at 42,920 and 44,310 cm^{-1}. The assignments given in Table II are again based on an intensity scheme. The band at 41,410 cm^{-1} in the low-temperature EPA spectrum is assigned to a d–d transition while the shoulder resolved at 41,920 cm^{-1} is assigned as $^1A_{1g} \rightarrow {}^1B_{1u}$. The shoulder at 44,310 cm^{-1} and the maximum at 45,090 cm^{-1} are assigned to $^1A_{1g} \rightarrow c^1E_u$, whereas the 46,190-cm^{-1} band is $^1A_{1g} \rightarrow {}^1A_{2u}$. An additional band is observed at 49,000 cm^{-1} in the aqueous solution spectrum of $Pd(CN)_4^{2-}$. This band is assigned as $^1A_{1g} \rightarrow d^1E_u$.

Square-Planar Ammine Complexes. The spectra of $Pd(NH_3)_4^{2+}$, $Pt(NH_3)_4^{2+}$, and $Au(NH_3)_4^{3+}$ in acetonitrile at room temperature are presented in Figure 5. Low-temperature measurements on these cationic complexes were not possible because of their extremely poor solubility in the glass-forming media. The acetonitrile spectra of $Pt(NH_3)_4^{2+}$ and $Au(NH_3)_4^{3+}$, however, represent a very marked improvement in resolution over the aqueous solution spectra. Band positions and assignments are summarized in Table III.

From the difference in the spectrochemical strengths of ammonia and chloride in several third-row octahedral complexes,[33] a shift of the first spin-allowed transition,

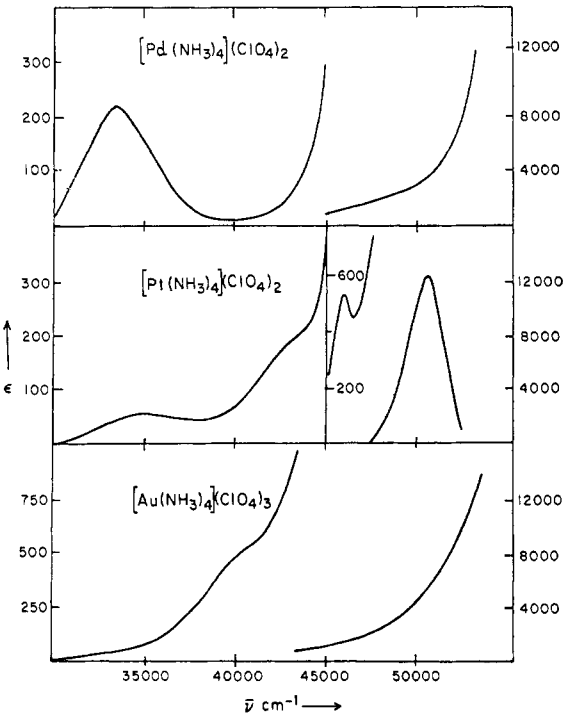

Figure 5. Electronic spectra of $[Pd(NH_3)_4](ClO_4)_2$, $[Pt(NH_3)_4](ClO_4)_2$, and $[Au(NH_3)_4](ClO_4)_3$ in CH_3CN at 24°.

$^1A_{1g} \rightarrow {}^1A_{2g}$, by about 18,000 cm^{-1} to higher energy for the ammine complex is expected. The $^1A_{1g} \rightarrow {}^1A_{2g}$ transition in $PtCl_4^{2-}$ is observed at about 25,000 cm^{-1}, and therefore the corresponding transition in $Pt(NH_3)_4^{2+}$ is expected at about 43,000 cm^{-1}. Conse-

(33) Reference 32, Chapter 15.

Table III. Electronic Spectra of Square-Planar Ammine Complexes[a]

H_2O	CH_3CN	$^1A_{1g} \rightarrow$
	$[Pd(NH_3)_4](ClO_4)_2$	
33.67 (180)	33.55 (212)	$^1A_{2g}$, ^1E_g, $^1B_{1g}$
>54.00	>53.00	$c\,^1E_u$
	$[Pt(NH_3)_4](ClO_4)_2$	
34.97 (42.5)	34.60 (54)	^3E_g, $^3A_{2g}$
41.66 (143)[b]	43.10 (191)[b]	$^1A_{2g}$, ^1E_g
45.25 (443)[b]	46.08 (560)	$^1B_{1g}$
50.76 (11,070)	50.50 (12,300)	$c\,^1E_u$
	$[Au(NH_3)_4](ClO_4)_3$	
...	40.32 (500)[b]	$^1A_{2g}$, ^1E_g

[a] $\bar{\nu} \times 10^{-3}$ cm^{-1} (ϵ, l. mole^{-1} cm^{-1}). [b] Shoulder (ϵ is for value of $\bar{\nu}$ given).

quently, the band observed in the $Pt(NH_3)_4^{2+}$ spectrum at 34,600 cm^{-1} must be assigned to a spin-forbidden d–d transition. With a simple σ-donor ligand such as NH_3, there should be very little difference in the energies of the $b_{2g}(xy)$ and $e_g(xz, yz)$ levels. Thus the band at 43,100 cm^{-1} is assigned as a combination of $^1A_{1g} \rightarrow {}^1A_{2g}$ and $^1A_{1g} \rightarrow {}^1E_g$, whereas the maximum at 46,080 cm^{-1} is assigned as $^1A_{1g} \rightarrow {}^1B_{1g}$.

In contrast to the $Pt(NH_3)_4^{2+}$ spectrum, only one broad band is observed for $Pd(NH_3)_4^{2+}$ below 53,000 cm^{-1}; this band is centered at 33,500 cm^{-1} in acetonitrile. In view of the extinction coefficient of this band it must be assigned as all three spin-allowed d–d transitions.[34] This would indicate that the $a_{1g}(z^2)$ level has moved to higher energy relative to the $Pt(NH_3)_4^{2+}$ case.

The aqueous solution spectrum of $Au(NH_3)_4^{3+}$ is very poorly resolved, and it is difficult to visualize any shoulders that correspond to low-energy electronic transitions. In contrast, the acetonitrile spectrum shows a distinct shoulder at 40,320 cm^{-1}. This transition is assigned to $^1A_{1g} \rightarrow {}^1A_{2g}, {}^1E_g$ by analogy to the platinum(II) complex. The transition is some 3000 cm^{-1} lower in energy for the gold(III) complex than for the platinum(II) complex. It is noteworthy that recent studies[14] on the $AuCl_4^-$ and $PtCl_4^{2-}$ complexes also place the first spin-allowed transition lower by about 3200 cm^{-1} in the gold(III) case.

At higher energy, a single intense band is observed at 50,500 cm^{-1} for $Pt(NH_3)_4^{2+}$. Corresponding bands in the $Pd(NH_3)_4^{2+}$ and $Au(NH_3)_4^{3+}$ spectra are indicated, but at energies greater than 53,000 cm^{-1}. This distinct red shift in the platinum(II) complex with respect to the palladium(II) and gold(III) complexes indicates that the logical assignment of the band at 50,500 cm^{-1} in the $Pt(NH_3)_4^{2+}$ spectrum is a d $\rightarrow$ p transition. The formal assignment suggested is $e_g(xz, yz) \rightarrow a_{2u}$-($^1A_{1g} \rightarrow c\,^1E_u$).

Discussion

Ligand-Field Parameters. Table IV summarizes the values of the ligand-field parameters, Δ_1, Δ_2, and Δ_3, derived from the d–d spectra of the complexes under investigation. The d–MO splitting pattern with

Table IV. Ligand-Field Parameters for Square-Planar Complexes[a]

Complex	Δ_1	Δ_2	Δ_3
$[PdCl_4]$ in $Pd_2Cl_6^{2-}$	25,920	4240	*b*
$[PdBr_4]$ in $Pd_2Br_6^{2-}$	20,450	3970	*b*
$PtCl_4^{2-}$	28,250	6250	8030
$PtBr_4^{2-}$	26,650	5230	3650
$AuCl_4^-$	25,430	6090	*b*
$AuBr_4^-$	22,090	4230	*b*
$Pd(NH_3)_4^{2+}$	37,050	1500	500
$Pt(NH_3)_4^{2+}$	46,600	1500	3480
$Au(NH_3)_4^{3+}$	43,800	*b*	*b*
$Ni(CN)_4^{2-}$	33,800	*b*	*b*
$Pd(CN)_4^{2-}$	44,600	*b*	*b*
$Pt(CN)_4^{2-}$	>50,000	*b*	*b*
$Au(CN)_4^-$	>50,000	*b*	*b*

[a] Energies in cm^{-1} for interelectronic-repulsion parameter values $B = 500$, $C = 3500$ cm^{-1}. [b] Insufficient data.

the $b_{1g}(x^2 - y^2)$ level considerably more unstable than the four occupied levels is well established. The values of Δ_1 are found to be larger than Δ_2 and Δ_3 combined (where data are available). Furthermore, the magnitude of Δ_1 for a given metal varies with the nature of the ligand in the order $CN^- > NH_3 > Cl^- > Br^-$. This ordering is consistent with the placement of these ligands in the octahedral spectrochemical series. The size of Δ_1 depends on the relative energies of the $b_{1g}(x^2 - y^2)$ σ^* and $b_{2g}(xy)$ π^* levels and, therefore, both d orbital σ and π bonding are contributing factors. For example, the π-acceptor cyanide ligand causes stabilization of the $b_{2g}(xy)$ level by $d\pi \rightarrow \pi^*CN$ interaction. The simple σ donor NH_3 ligand causes a marked destabilization of the $b_{1g}(x^2 - y^2)$ level while the $b_{2g}(xy)$ level remains essentially nonbonding. The halides are weak σ donors but good π donor ligands and will destabilize the $b_{2g}(xy)$ level with respect to $b_{1g}(x^2 - y^2)$.

Table IV shows that Δ_1 increases very markedly in the order Ni(II) < Pd(II) < Pt(II) for CN^- as ligand. The strong increase is similar to that observed[26] for the octahedral cyanides of Co(III), Rh(III), and Ir(III) and may be interpreted[35] as increasing σ bonding in the order $3d\sigma < 4d\sigma < 5d\sigma$. It is of interest that the Δ results for cyanide complexes in the Ni and Co families contrast with the slow increase in Δ in the Fe family cyanides.[26] Apparently, the relatively contracted $5d\sigma$ orbitals of Ir(III) and Pt(II) are better suited for σ bonding than are the larger $5d\sigma$ orbitals of Os(III). We have previously argued that a relatively contracted $5d\sigma$ orbital may give better $d\sigma$ overlap than a more expanded one because of the cancelling effect of nodes in the latter situation.

There is a limit, however, to the degree to which contraction will aid $5d\sigma$ overlap. The data in Table IV show clearly that in every case $\Delta_1[Pt(II)] > \Delta_1[Au(III)]$, as predicted from molecular orbital calculations.[4] The fact that this "inverse" relationship holds even for a simple σ donor ligand such as NH_3 indicates that d orbital σ bonding *decreases* in going from Pt(II) to

(34) Magnetic circular dichroism measurements performed by A. J. McCaffery and P. N. Schatz at the University of Virginia indicate that the 33,550-cm^{-1} band in $Pd(NH_3)_4^{2+}$ shows a small but distinct *A* term. This is consistent with a degenerate excited state for the transition(s) involved.

(35) The alternative interpretation, involving increasing d $\rightarrow \pi^*CN$ bonding ($3d < 4d < 5d$), may be ruled out in this case because infrared spectra of $[(n\text{-}C_4H_9)_4N]_2[M(CN_4)]$ in acetonitrile show[36] $\bar{\nu}(C{\equiv}N)$ *higher* in both $Pd(CN)_4^{2-}$ (2127 cm^{-1}) and $Pt(CN)_4^{2-}$ (2121 cm^{-1}) than in $Ni(CN)_4^{2-}$ (2113 cm^{-1}).

Table V. Charge-Transfer Energies for Halide Complexes

Complex[b]	Lπ → dσ* system[a] $^1A_{1g} \rightarrow a^1T_{1u}, b^1T_{1u}$	Lσ → dσ* system $^1A_{1g} \rightarrow c^1T_{1u}$
$RhCl_6^{3-}$	41,000	...
$RhBr_6^{3-}$	28,600	38,600
$IrCl_6^{3-}$	48,500	...
$IrBr_6^{3-}$	37,000 (41,500)	...
$PdCl_6^{2-}$	29,400	41,700
$PtCl_6^{2-}$	37,700[c]	49,200[c]
$PtBr_6^{2-}$	30,580, 31,540[c]	44,400[c]
	$^1A_{1g} \rightarrow {}^1A_{2u}, a^1E_u$	$^1A_{1g} \rightarrow b^1E_u$
[$PdCl_4$] in $Pd_2Cl_6^{2-}$	34,700[d]	~50,000[d]
[$PdBr_4$] in $Pd_2Br_6^{2-}$	30,720[d]	46,300[d]
$PtCl_4^{2-}$	43,670, 46,300[e]	>54,000
$PtBr_4^{2-}$	33,330, 36,040	47,380
$AuCl_4^-$	31,050	44,250
$AuBr_4^-$	25,250	39,060

[a] Energies in cm^{-1}. [b] Data for MX_6^{n-} taken from ref 32, except as indicated. [c] From ref 36. [d] $L_T \rightarrow M$. [e] See ref 28.

Au(III). Thus it appears that maximum 5dσ overlap occurs for Ir(III) and Pt(II) and is somewhat lower for both Os(III) and Au(III).

Charge-Transfer Energies. Table V compares L→M charge-transfer energies in d^6 octahedral[32,36] and d^6 square-planar halide complexes. It is notable that the charge-transfer band system in the square-planar Pd(II) and Pt(II) complexes is observed at higher energy than the band system in the octahedral Pd(IV) and Pt(IV) complexes. The trend is expected because of the lower stability of the M(II) metal orbitals. The importance of metal orbital stability in determining charge-transfer energies is further shown by the 9250-cm^{-1} shift to higher energy of the first L→M band in going from $PdCl_4^{2-}$ to $PtCl_4^{2-}$. This shift is substantially larger than the corresponding Δ_1 change of 2300 cm^{-1}; it must, therefore, be largely due to the difference in atomic 4d and 5d orbital energies.

In all cases the bromo complex shows lower energy charge transfer than does the corresponding chloro complex as expected from ligand orbital stability, but the difference in charge-transfer energy between these two ligands is dependent on the metal; for example, the difference between MCl_4^{n-} and MBr_4^{n-} for Pd(II) is 4000 cm^{-1}; Au(III), 5800 cm^{-1}; Pt(II), 10,340 cm^{-1}. The increase in difference parallels the decrease in metal orbital stability, but it is not at all clear why bromide and chloride should be so differently affected.

From Table V it appears that a two-band L→M charge-transfer system with a separation of 10,000–16,000 cm^{-1} is characteristic of both octahedral MX_6^{n-} and square-planar MX_4^{n-} halide complexes. The lower energy band is assigned to $L\pi \rightarrow d\sigma^*$ while the higher energy transition is assigned to $L\sigma \rightarrow d\sigma^*$. The resolution of the lower energy band into two components, $^1A_{1g} \rightarrow {}^1A_{2u}$ and $^1A_{1g} \rightarrow a^1E_u$ in the case of PtX_4^{2-}, establishes the fact that the ligand π levels are indeed at higher energy than ligand σ levels. The assignments of the two transitions indicate relative stability for the $e_u\pi$ level; this may be taken as evidence of the importance of the participation of the 6p orbital in bonding in Pt(II) complexes.

Table VI compares M→L charge-transfer energies of d^6 octahedral[26] and d^6 square-planar cyanide complexes. The transitions to the $a_{2u}\pi^*$ CN level of the

(36) W. R. Mason, unpublished results, 1967.

Table VI. Charge-Transfer Energies for Cyanide Complexes in Aqueous Solution[a]

$M(CN)_6^{n-}$ complex[b]	$^1A_{1g} \rightarrow c^1T_{1u}$	$M(CN)_4^{n-}$ complex	$^1A_{1g} \rightarrow c^1E_u$	$^1A_{1g} \rightarrow d^1E_u$
$Fe(CN)_6^{4-}$	45,870	$Ni(CN)_4^{2-}$	37,300	50,500
$Ru(CN)_6^{4-}$	48,500	$Pd(CN)_4^{2-}$	45,450	49,000
$Os(CN)_6^{4-}$	47,950	$Pt(CN)_4^{2-}$	39,000	46,190
$Co(CN)_6^{3-}$	49,500[d]	...		
$Rh(CN)_6^{3-}$	>50,000	...		
$Ir(CN)_6^{3-}$	>50,000	$Au(CN)_4^-$	>54,000	>54,000

[a] Energies in cm^{-1}. [b] Data for $M(CN)_6^{n-}$ taken from ref 26.

$M(CN)_4^{n-}$ complexes, $^1A_{1g} \rightarrow c^1E_u$, are observed at lower energies than the M→L transitions of the $M(CN)_6^{n-}$ complexes of either the Fe(II) or Co(III) group. This shift to lower energy is attributed to the increased importance of the a_{2u} *n*p metal orbital in square-planar systems. The transitions to the $e_u\pi^*$ CN orbital in the planar systems, on the other hand, are observed at energies more comparable to those of the $M(CN)_6^{n-}$ complexes; the $e_u\pi^*$ CN level is not as sensitive to the metal as the a_{2u} level and the observed energies are about what would be expected by extrapolation from the Co(III) family. Furthermore, the c^1E_u energy ordering of Au(III) > Pt(II) < Pd(II) can be explained in terms of the expected increased participation of the 6p over 5p orbitals. Direct evidence for the lower $6p(a_{2u})$ than $5p(a_{2u})$ level is obtained from the d → p spectra of $Pt(NH_3)_4^{2+}$ and $Pd(NH_3)_4^{2+}$. In the latter case the transition $b_{1g}(xy) \rightarrow a_{2u}(5p)$ comes at higher energy than the $b_{2g}(xy) \rightarrow a_{2u}(6p)$ transition in the former complex.

The movement of the $a_{1g}(z^2)$ level with respect to the other occupied d levels in the series Ni(II), Pd(II), and Pt(II) can be described from the charge-transfer data of the $M(CN)_4^{2-}$ complexes. In $Ni(CN)_4^{2-}$, the $a_{1g}(z^2)$ level is approximately 2000 cm^{-1} more energetic relative to the $e_g(xz, yz)$ level than it is in $Pd(CN)_4^{2-}$; and it is 3200 cm^{-1} higher in the same comparison with $Pt(CN)_4^{2-}$. It is not likely that the small differences in interelectronic repulsion among these complexes will alter this trend.

A similar movement of the $a_{1g}(z^2)$ level is observed from the Δ_3 values of $Pd(NH_3)_4^{2+}$ and $Pt(NH_3)_4^{2+}$; the $a_{1g}(z^2)$ level is about 500 cm^{-1} below $e_g(xz, yz)$ in Pd(II) and moves to about 3500 cm^{-1} below $e_g(xz, yz)$ in Pt(II). Thus the $a_{1g}(z^2)\sigma^*$ level is a stronger function of the period in complexes of ammine ligands than in the cyanide case. Although no quantitative data are available for Δ_3 values of the Pd(II) halide complexes, it is probable that a similar trend would be found for halide ligands.

The fact that $a_{1g}(z^2)$ becomes less antibonding relative to the other d orbital levels on proceeding from Ni(II) to Pt(II) may be interpreted as due to increased participation of the valence s orbital in the $a_{1g}\sigma$ bonding. Presumably, *n*s bonding is very strong in the case of the 6s Pt(II) orbital; the result is less involvement of $5d_{z^2}$ and increased stability in $a_{1g}(z^2)$.

Acknowledgments. We thank the National Science Foundation for support of this research. Acknowledgment is due Professor P. N. Schatz and Dr. A. J. McCaffery for communicating results of magnetic circular dichroism measurements to us.